BI-DIRECTIONAL GRID CONSTRAINED STOCHASTIC PROCESSES' LINK TO MULTI-SKEW BROWNIAN MOTION

ALDO TARANTO, RON ADDIE, SHAHJAHAN KHAN

School of Sciences
University of Southern Queensland
Toowoomba, QLD 4350, Australia

ABSTRACT. Bi-Directional Grid Constrained (BGC) stochastic processes (BGC-SPs) constrain the random movement toward the origin steadily more and more, the further they deviate from the origin, rather than all at once imposing reflective barriers, as does the well-established theory of Itô diffusions with such reflective barriers. We identify that BGCSPs are a variant rather than a special case of the multi-skew Brownian motion (M-SBM). This is because they have their own complexities, such as the barriers being hidden (not known in advance) and not necessarily constant over time. We provide a M-SBM theoretical framework and also a simulation framework to elaborate deeper properties of BGCSPs. The simulation framework is then applied by generating numerous simulations of the constrained paths and the results are analysed. BGCSPs have applications in finance and indeed many other fields requiring graduated constraining, from both above and below the initial position.

CONTENTS

NOTATION

Term	Description
BGC	Bi-Directional grid constrained
BGCSP	BGC stochastic process
M-SBM	Multi-skew Brownian motion
X_t	Stochastic process over time t
B_t	Brownian motion over time t
W_t	Wiener process over time t
T	Time
$f(X_t, t)$, μ	Drift coefficient of X over t
$g(X_t, t)$, σ	Diffusion coefficient of X over t
$\Psi(X_t, t)$	BGC coefficient of X over t
$\text{sgn}[X_t]$	Sign function of X_t
$\mathfrak{B}_L$	Lower barrier
$\mathfrak{B}_U$	Upper barrier
$\tau_{\mathfrak{B}}$	Stopping time when $\mathfrak{B}$ is hit
$|x|$	Absolute value of x

1. INTRODUCTION

In Taranto et al. [33], the concept of Bi-Directional Grid Constrained (BGC) sto-
chastic processes (BGCSPs) was introduced, and the impact of BGC on the iterated
logarithm bounds of the corresponding stochastic differential equation (SDE) was
derived. In the subsequent paper (Taranto and Khan [32]), the hidden geometry
of the BGC process was examined, in particular how the hidden reflective barriers
are formed, the various possible formulations that can be formed, and an algorithm
to simulate BGCSPs was provided. BGCSPs were also compared to the Langevin
equation, the Ornstein-Uhlenbeck process (OUP), and it was shown how BGCSPs
are more complex due to a more general framework that does not always admit an
exact solution. In this paper, we examine in what respects a BGCSP resembles and
in what respect it differs from a type of multi-skew Brownian motion (M-SBM).

Before we do this, we recall that the BGC term $\text{sgn}[X_t]\Psi(X_t, t)$, from now onwards
simply $\Psi(X_t, t)$, unless required to be fully expressed, has been defined as impacting
the dt term as in [33] or the dW_t term to a lesser extent as in [32]. Here, we notice
that even if this term is placed as a factor outside the sum of the dt and dW_t terms,
it will still constrain the Itô diffusion in a slightly different, yet fundamentally the
same way. Since $\Psi(x)$ is continuous and differentiable, we require $\Psi(x)$ to include
the infinitessimal d, giving $d\Psi(x)$. We thus provide the following third alternative
definition of the BGCSP.

Definition 1.1. *(Definition III of BGC Stochastic Processes). For a complete filtered probability space $(\Omega, \mathcal{F}, \{\mathcal{F}\}_{t \geqslant 0}, \mathbb{P})$ and a (continuous) BGC function $\Psi(x) : \mathbb{R} \rightarrow \mathbb{R}$, $\forall x \in \mathbb{R}$, $f(X_t, t)$ is the drift coefficient, $g(X_t, t)$ is the diffusion coefficient, $\Psi(X_t, t)$ is the BGC function. $f(X_t, t)$, $g(X_t, t)$ and $\Psi(X_t, t)$ are convex functions and $\mathrm{sgn}[x]$ is the sign function defined in the usual sense,*

$$
\mathrm{sgn}[x] \quad = \quad \left\{ \begin{array}{ccc} 1 & , & x > 0 \\ 0 & , & x = 0 \\ -1 & , & x < 0 \end{array} \right. .
$$

Then, the corresponding BGC Itô diffusion is defined as follows,

$$
dX_t = f(X_t, t)\, dt + g(X_t, t)\, dW_t - \underbrace{\mathrm{sgn}[X_t]\, d\Psi(X_t, t)}_{BGC}. \tag{1.1}
$$

∎

By choosing $\Psi(X_t, t)$ to be a 'suitable' parabolic cylinder function in relation to the underlying Itô diffusion, as shown in [32], namely $\Psi(X_t, t) = \left(\frac{X_t}{10}\right)^2$, the hidden barriers become visible when enough simulations hit them. Figure 1 shows that (1.1) is simulated 1,000 times for both with and without BGC, together with the hidden lower reflective barrier $a = \mathfrak{B}_L$ and the hidden reflective upper barrier $b = \mathfrak{B}_U$ also being displayed.
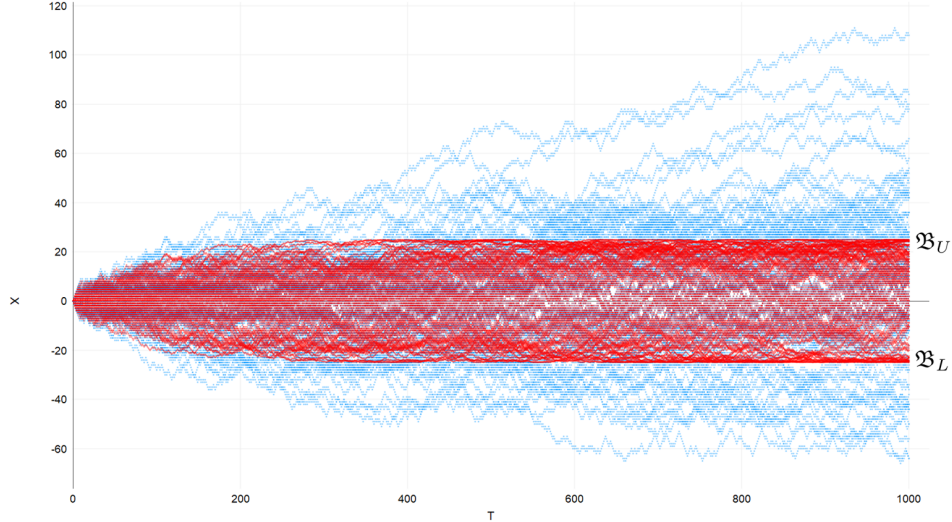

FIGURE 1. Hidden Reflective Barriers due to Ideal $\Psi(X_t, t)$

Blue = Unconstrained Itô process, Red = BGC Itô process. Even though there are no hard reflective barriers present, the function $\Psi(X_t, t)$ constrains the Itô process 'as if' there are two hidden reflective barriers $\mathfrak{B}_L$, $\mathfrak{B}_U$.

An even more specialized case that is of great interest, due to its simplicity, is where drift function $f(x) : \mathbb{R} \to \mathbb{R}$ is set to $f(x) = \mu$, $\forall x \in \mathbb{R}$ and similarly, the diffusion function $g(x) : \mathbb{R} \to \mathbb{R}$ is set to $g(x) = \sigma$, $\forall x \in \mathbb{R}$. One can even define $f(x)$ and $g(x)$ in a more gradual manner such that in the limit they approach the typical constant expressions for the drift and diffusion coefficients,

$$\lim_{x \to \infty} f(x) = \mu \quad , \quad \lim_{x \to \infty} g(x) = \sigma. \tag{1.2}$$

Depending on whether the generalized $f(x)$ and $g(x)$ are used, or whether the simplified μ and σ are used, then the resulting reflective boundary theorems will either have more complexity, or less complexity, respectively.

Before proceeding to the Methodology section, (1.1) is discussed within a multi-Dimensional context with some examples, which will help explain the multidimensionality of M-SBMs.

Remark 1.2. *By multi-Dimensional diffusion, we are not referring to the usage in papers such as Sacerdote et al. [27] in which each dimension is reserved for each possible path or simulation, as shown in Figure 2(a).*

(a).   *(b).*
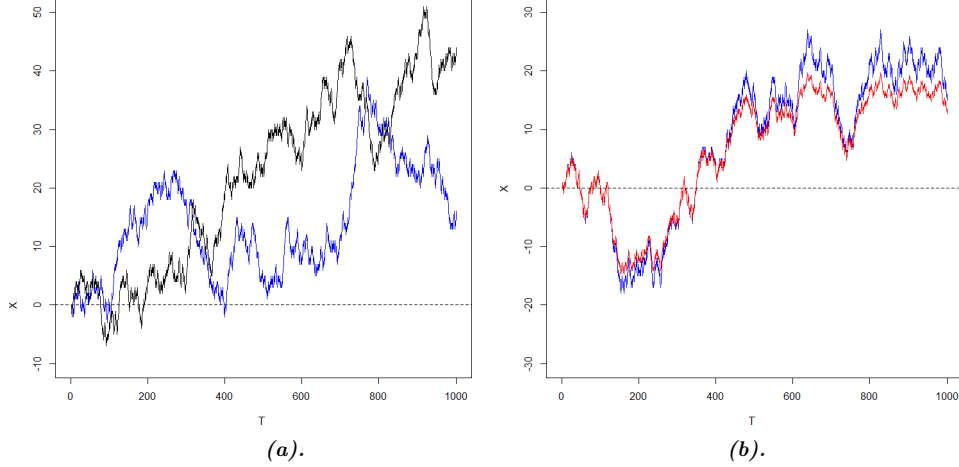
FIGURE 2. Clarifying Subtle Differences for BGC Stochastic Processes

(a). Two unconstrained 1-D Itô diffusions are not considered in this paper as one 2-D Itô diffusion.

(b). Blue = Unconstrained Itô diffusion, Red = BGC Itô diffusion, noting that the BGC process exhibits a 'skew' above and below and can be considered as a 2-SBM.

Notice that in Figure 2(b), the BGCSP exhibits a 'skew' and can be considered as a 2-SBM -which will be elaborated in the Methodology section. Instead of the usage in Figure 2(a), we use the standard interpretation and generally accepted usage of

(a). *2-D Itô Diffusion as seen from X*   (b). *2-D Itô Diffusion as seen from Y*

FIGURE 3. 2-Dimensional Itô Diffusion as seen from 2 Different Dimensions

The colour scale is a hot to cold measure indexed on the time variable t in dimension T for $t \in [0, 1000]$.

the term 'multi-Dimensional diffusion' in which each dimension is reserved for each co-ordinate of the multivariate Itô process, as shown in Figure 3.

We also note that the Methodology, Results and Discussion sections are either directly multi-Dimensional or can be extended to multi-Dimensional expressions.

∎

We now have a more geometric understanding of how BGCSPs can be constrained along multiple dimensions, to be in a better position to express (1.1) in a more generalized n-Dimensional framework in (1.3).

Definition 1.3. *(Definition IV - Multi-Dimensional BGC Stochastic Processes). Let $X : [0, \infty) \times \Omega \to \mathbb{R}^n$ defined on a probability space $(\Omega, \mathcal{F}, \{\mathcal{F}\}_{t \geqslant 0}, \mathbb{P})$ be an Itô diffusion satisfying the conditions given in the definition of the 1-Dimensional Itô process for each $\{1 \leqslant i \leqslant n\}$, $\{1 \leqslant j \leqslant m\}$, then we can form n 1-Dimensional Itô processes in an SDE of the form,*

$$
\begin{aligned}
dX_1 \quad = \quad & f_1(X_t, t)\, dt + \underbrace{g_{1,1}(X_t, t)\, dW_1(t) + \cdots + g_{1,m}(X_t, t)\, dW_m(t)}_{m} \\
& - \underbrace{\mathrm{sgn}[X_t]\, d\Psi_1(X_t, t) - \ldots - \mathrm{sgn}[X_t]\, d\Psi_m(X_t, t)}_{m\ BGC} \\
\vdots \quad \vdots \quad & \qquad\qquad\qquad\qquad \vdots \\
dX_n \quad = \quad & f_n(X_t, t)\, dt + \underbrace{g_{n,1}(X_t, t)\, dW_1(t) + \cdots + g_{n,m}(X_t, t)\, dW_m(t)}_{m} \\
& - \underbrace{\mathrm{sgn}[X_t]\, d\Psi_1(X_t, t) - \ldots - \mathrm{sgn}[X_t]\, d\Psi_m(X_t, t)}_{m\ BGC}
\end{aligned}
\tag{1.3}
$$

where $W_t = (W_1(X_t, t), ..., W_m(X_t, t))$ is an m-Dimensional Wiener process and $f : \mathbb{R}^n \to \mathbb{R}^n$ and $g : \mathbb{R}^n \to \mathbb{R}^{n \times m}$ are the drift and diffusion fields respectively. For

a point $x \in \mathbb{R}^n$, let $\mathbb{P}^x$ denote the law of X given initial datum $X_0 = x$, and let $\mathbb{E}^x$ denote expectation with respect to $\mathbb{P}^x$. Now, (1.3) can also be expressed in matrix notation as,

$$d\mathbf{X}_t = \boldsymbol{f}_t\, dt + \boldsymbol{g}_t\, d\mathbf{W}_t - \boldsymbol{h}_t, \tag{1.4}$$

where,

$$\mathbf{X}_t = \begin{pmatrix} dX_1(t) \\ \vdots \\ dX_n(t) \end{pmatrix}, \ \boldsymbol{f}_t = \begin{pmatrix} f_1(X_t, t) \\ \vdots \\ f_n(X_t, t) \end{pmatrix}, \ \boldsymbol{g}_t = \begin{pmatrix} g_{1,1}(X_1(t), t) & \cdots & g_{1,m}(X_1(t), t) \\ \vdots & \ddots & \vdots \\ g_{n,1}(X_n(t), t) & \cdots & g_{n,m}(X_n(t), t) \end{pmatrix},$$

$$d\mathbf{W}_t = \begin{pmatrix} dW_1(t) \\ \vdots \\ dW_n(t) \end{pmatrix}, \ \boldsymbol{h}_t = \begin{pmatrix} \mathrm{sgn}[X_1(t)]\, d\Psi_1(X_1(t), t) \\ \vdots \\ \mathrm{sgn}[X_n(t)]\, d\Psi_n(X_n(t), t) \end{pmatrix},$$

for vectors $\boldsymbol{f}_t$, $\boldsymbol{h}_t$, $\boldsymbol{W}_t$ and matrix $\boldsymbol{g}_t$. ∎

Having reviewed the multi-Dimensional nature of unconstrained and BGC Itô diffusions, the paper is structured as follows; Section 2 provides the Literature Review, Section 3 the Methodology, Section 4 the Results and Discussion, and finally, Section 5 the Conclusion.

2. Literature Review

2.1. **Constraining Stochastic Processes by Reflective Barriers.** The constraining of stochastic processes in the form of discrete random walks and continuous Wiener processes has been researched for many decades. By reviewing Weesakul [34] and the references therein, we see an established and rigorous analysis of random walks between a reflecting and an absorbing barrier. Lehner [16] extended this to 1-Dimensional random walks with a partially reflecting (semipermeable) barrier. Gupta [9] generalised this concept further to random walks in the presence of a multiple function barrier (MFB) where the barrier can either be partially reflective, absorptive, transmissive or hold for a moment, but not terminating or killing the random variable. Dua et al. [7] extended the work of [16] to random walks in the presence of partially reflecting barriers in which the probability of a random variable or datum reaching certain states was determined. Lions and Sznitman [20] extended the research on reflecting boundary conditions through the refinement to SDEs. Percus [24] considered an asymmetric random walk, with one or two boundaries, on a 1-Dimensional lattice. At the boundaries, the walker is either absorbed or reflected back to the system. Budhiraja and Dupuis [5] considered the large deviation properties of the empirical measure for 1-Dimensional constrained processes, such as reflecting Wiener processes, the M/M/1 queue, and discrete-time analogs. L'epingle [18] examined stochastic variational inequalities to provide a unified treatment for SDEs existing in a closed domain with normal reflection and (or) singular repellent drift. When the domain is a polyhedron, he proved that the reflected-repelled Wiener process does not hit the non-smooth part

of the boundary. Bramson et al. [4] examined the positive recurrence (to the origin) of reflecting Wiener processes in 3-Dimensional space. Ball and Roma [3] examined the detection of mean reversion within reflecting barriers with an application to the European exchange rate mechanism (EERM).

2.2. **Multi-Skew Brownian Motion.** The concept of skew Brownian motion (SBM) was first introduced in the book by Itô and McKean [13] as a diffusion with a drift represented by a generalized function, which solves an SDE involving its symmetric local time. Specifically, an SBM $X = \{X_t\}_{t \in [0,T]}$ is the solution of,

$$X_t = B_t + (2\alpha - 1)L_t^0(X), \quad \alpha \in (0,1),$$

where $B = \{B_t\}_{t \in [0,T]}$ is a standard Brownian motion (BM). However, standard Brownian motion is oftentimes abbreviated as SBM, so to reduce any possible confusion and to eliminate any reference to the original botanical context of Robert Brown -to which the term 'Brownian motion' is attributed -we will express B_t in the rest of this paper in the more mathematically precise context as a Wiener process $W = \{W_t\}_{t \in [0,T]}$. $L_t^0(X) = \lim_{\epsilon \downarrow 0} \frac{1}{2\epsilon} \int_0^t \mathbb{1}_{\{|B_{X_s}| \leqslant \epsilon\}} \, ds$ is the symmetric local time at X_0. Note that for $\alpha = \frac{1}{2}$, the above equation is reduced to a Wiener process. Harrison and Shepp [10] then considered diffusions with a discontinuous local time. The literature on SBMs was consolidated by Harrison and Shepp [10] and later by Lejay [17]. Applications of SMBs were extended by Ramirez [26] by applying multi-SBM (M-SBM) and diffusions in layered media that involve advection flows. Appuhamillage and Sheldon [1] linked SBMs to existing research by deriving the first passage time (FPT) of SBM. In 2015, the multiple barrier research of [26] was extended by Atar and Budhiraja [2], Ouknine et al. [23] who collapsed barriers to an accumulation point, and by Dereudre et al. [6] who derived an explicit representation of the transition densities of SBM with drift and two semipermeable barriers. Mazzonetto [21] extended her prior research [6] on SBMs by deriving exact simulations of SBMs and M-SBMs with discontinuous drift in her Doctoral dissertation. Gairat and Shcherbakov [8] applied SBMs and their functionals to finance. Krykun [14] also extended the convergence of SBM with local times at several points that are contracted into a single one. Mazzonetto [22] has also recently examined the rates of convergence to the local time of oscillating and SBMs.

For applications of BGC stochastic processes, the reader is referred to [30], [28], [29], [31].

3. Methodology

Before proceeding to the main result of this paper, it is instructive to establish a theoretical foundation by considering the key research for Itô diffusions constrained by two reflective barriers and then examining the necessary extensions that need to be derived for M-SBM constrained Itô diffusions.

3.1. **Itô Diffusions Constrained by Two Reflective Barriers.** Given a filtered probability space $\Lambda := (\Omega, \mathcal{F}, \{\mathcal{F}_t\}_{t \geqslant 0}, \mathbb{P})$ with the filtration $\{\mathcal{F}_t\}_{t \geqslant 0}$, then the reflected diffusion $\{X_t : t \geqslant 0\}$ with two-sided barriers $\mathfrak{B}_L, \mathfrak{B}_U$ at a, b respectively can be defined as,

$$dX_t = f(X_t) \, dt + g(X_t) \, dW_t + \underbrace{\overbrace{d\mathcal{A}_t}^{a} - \overbrace{d\mathcal{B}_t}^{b}}_{\text{regulators}}, \quad X_0 \in (a, b), \quad x \in [a, b]. \qquad (3.1)$$

Remark 3.1. *The process $\mathcal{A}$ and $\mathcal{B}$ are known in the literature as 'regulators' for the points a and b, however, we believe that a better term is 'detectors' because they mainly detect or count how many times X_t reaches a and b.*

Here, the drift $f(x)$ is Lipschitz continuous, the diffusion $g(x)$ is strictly positive and Lipschitz continuous. a, b with $-\infty < a < b < +\infty$ are given real numbers, and $(W_t, 0 \leqslant t < \infty)$ is the 1-Dimensional standard Wiener process on Λ. The processes $\mathcal{A} = \{\mathcal{A}_t\}_{t \geqslant 0}$ and $\mathcal{B} = \{\mathcal{B}_t\}_{t \geqslant 0}$ are the minimal non-decreasing and non-negative processes, which restrict the process $X_t \in [a, b], \forall t \geqslant 0$. More precisely, the processes $\{\mathcal{A}_t, t \geqslant 0\}$ and $\{\mathcal{B}_t, t \geqslant 0\}$ increase only when X_t hits the boundary a and b, respectively, so that $\mathcal{A}_0 = \mathcal{B}_0 = 0$, $\mathbb{1}$ is the characteristic function of the set and,

$$\int_0^\infty \mathbb{1}_{\{X_t > a\}} \, d\mathcal{A}_t = 0, \quad \int_0^\infty \mathbb{1}_{\{X_t < b\}} \, d\mathcal{B}_t = 0. \qquad (3.2)$$

Furthermore, the processes $\mathcal{A}$ and $\mathcal{B}$ are uniquely determined by the following properties (Harrison [11]),

(1) both $t \to \mathcal{A}_t$ and $t \to \mathcal{B}_t$ are nondecreasing processes,
(2) $\mathcal{A}$ and $\mathcal{B}$ increase only when $X = a$ and $X = b$, respectively, that is $\int_0^t \mathbb{1}_{\{X_s = a\}} \, d\mathcal{A}_s = \mathcal{A}_t$ and $\int_0^t \mathbb{1}_{\{X_s = b\}} \, d\mathcal{B}_s = \mathcal{B}_t$, for $t \geqslant 0$.

We can consider the two reflective barriers as forming a 2-SBM. Furthermore, it is instructive for BGCSP to see the two barriers a and b in $\mathbb{R}^2$, shown in Figure 4(a) as embedded in $\mathbb{R}^3$ by a governing BGC surface $\Psi(X_t, t)$, as shown in Figure 4(b).

Remark 3.2. *Many papers such as [12] and Linetsky [19] define the two barriers at the boundaries of $[0, r]$ for some $r \in \mathbb{R}_+$. By applying a series of transformations, one can map their findings to the context of BGCSP, as shown in Figure 5.*
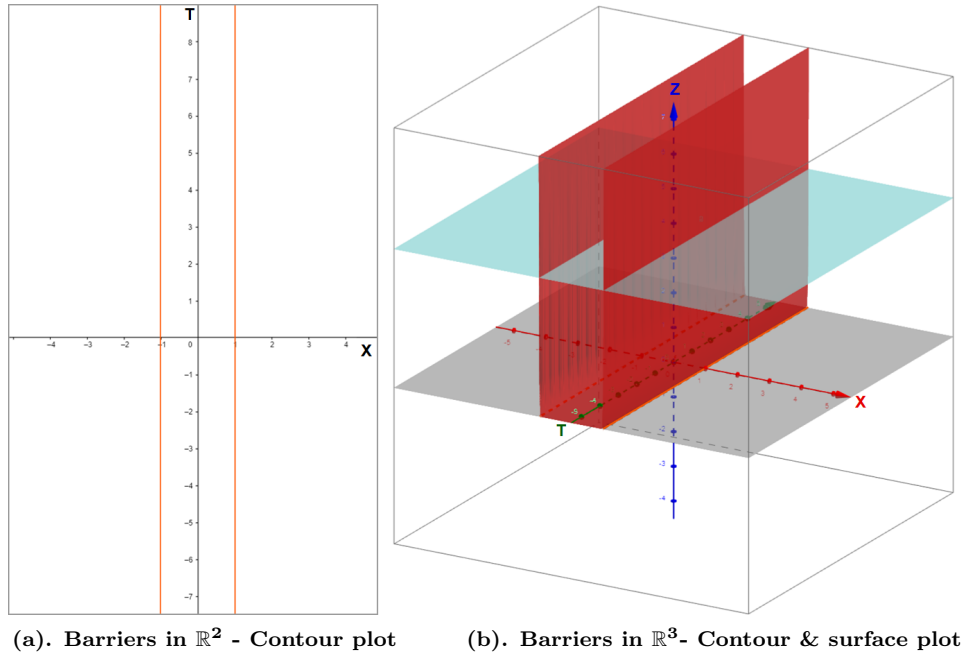
■

(a). Barriers in $\mathbb{R}^2$ - Contour plot   (b). Barriers in $\mathbb{R}^3$- Contour & surface plot

FIGURE 4. Diffusion Between Two Constant Reflective Barriers

As the light blue plane $z = k$ for $k \in \mathbb{R}_+$ descends to the origin, the orange contour lines of the red constant reflective barriers do not change. The contour lines arise from when the blue plane intersects the barrier surface in $\mathbb{R}^3$ that acts as two barriers in $\mathbb{R}^2$.
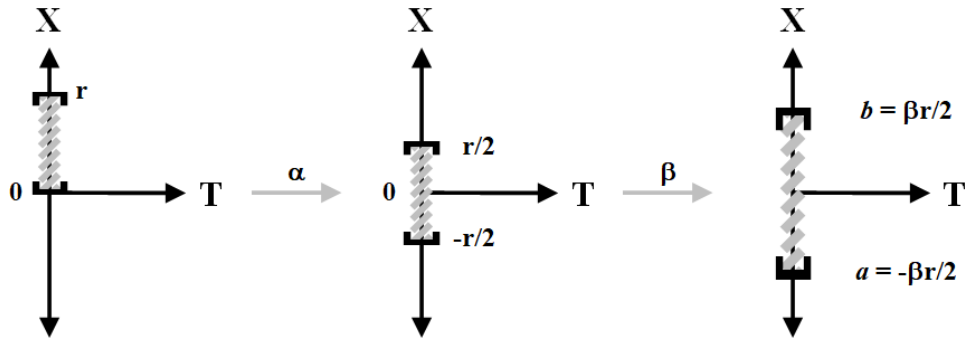

FIGURE 5. Mapping Traditional Barriers to BGC Barriers

By applying the transformations α and β to the barriers at 0 and r, the result is a linear combination of mappings with the same properties as the original for the barriers at a and b.

3.2. **Multi-Skew Brownian Motion.** Having examined Itô diffusions constrained by two reflective barriers, we now consider the so-called multi-skew Brownian motion, constrained by multiple barriers of varying degrees of reflectiveness.

Definition 3.3. *(M-SBM). A multi-skew Brownian motion (M-SBM) represented (adapted from Mazzonetto [21]) by $(\beta_1, ..., \beta_n)$-SBM, or more simply by β-SBM with n semipermeable barriers of varying permeability coefficients, respectively $\beta = (\beta_1, ..., \beta_n)$, x_0 is the starting position, the coefficients $\beta_j \in [-1, 1]$, barriers $x_1 < ... < x_n$, local times $L_t^{x_j}$, and $\mathcal{E}$ is the set of all parameters of the M-SBM, then the M-SBM is expressed as,*

$$\begin{cases} dX_t &=& \mu \, dt + \sigma \, dW_t + \beta_1 \, dL_t^{x_1} + ... + \beta_n \, dL_t^{x_n} \\ X_0 &=& x_0 \\ \mathcal{E} &=& \left\{ \mu, \sigma, (\beta_1, ..., \beta_n) \right\} \in \mathbb{R} \\ L_t^{x_j} &=& \int_0^t \mathbb{1}_{\{X_s = x_j\}} \, dL_s^{x_j}, \ \forall j \in \{1, ..., n\} \end{cases}.$$

∎

Remark 3.4. *The term σ has been added to the [21] definition so that the process can fit a wider range of models. We require that $\beta_i \in [-1, 1]$. The cases when $\beta_i = \{-1, 1\}$ are said to exhibit zero permeability (i.e. impermeability or full reflectiveness), and when $\beta_i \in (-1, 1)$ the process is said to exhibit partial reflectiveness (i.e. semi permeability). Note that a 0-SBM is simply a Wiener process and a $\pm$ 1-SBM is a positively/negatively reflected Wiener process. The definition of M-SBM is illustrated in Figure 6, representing a typical example of M-SBM. The standard definition of a skew Brownian motion has a drift term $\mu \in \mathbb{R}$ making it no longer, strictly speaking, Brownian motion.*
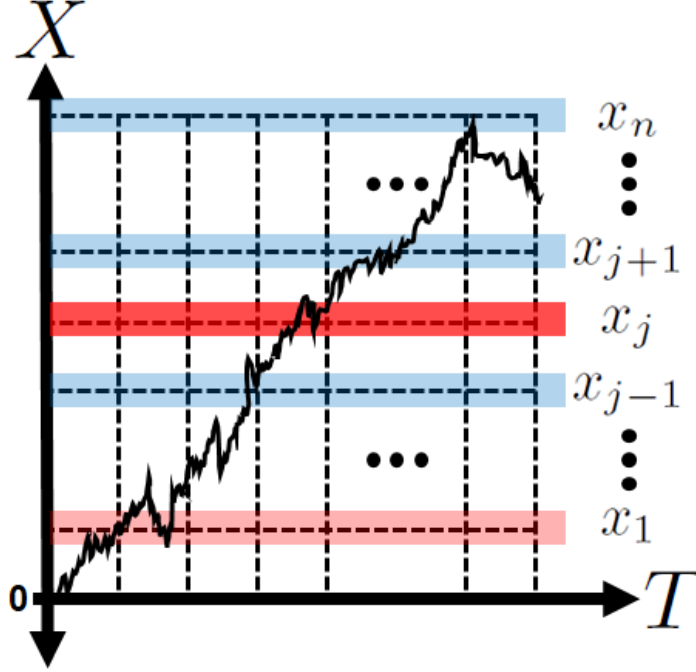
FIGURE 6. Example Standard M-SBM Framework

(a). Red barriers have permeability values $\beta_j < 0$ so reflect to the left (upwards). The more negative the value is within $\beta_j \in [-1, 0)$, the more reflective the barrier is (i.e. the less permeable it is).

(b). Blue barriers have permeability values $\beta_j > 0$ so reflect to the right (downwards). The more positive the value is within $\beta_j \in (0, 1]$, the more reflective the barrier (i.e. the less permeable it is).

(c). Barriers that have permeability values $\beta_j = 0$ are not depicted since they have no (constraining) effect.

The M-SBM of Definition 3.3 allows any barrier combination to be either fully reflective or semipermeable.

Remark 3.5. *If the permeability is $\beta_j = 1$ at the barrier x_j for some $j \in \{1, ..., j_1, j, j+ 1, ..., n\}$ and the initial position is $x_0 \in (x_j, +\infty)$, then the lower barriers $x_1, ..., x_{j-1}$ will almost surely be never reached [21]. For this to happen, it must be that $\beta_j = -1$, so that as the Itô diffusion descends (down) to x_j, it is fully reflected back (up). This of course assumes that the diffusion coefficient σ is 'relatively small' and so allows the Itô diffusion to be 'well behaved' and never 'jump over' and go below the x_j barrier, as also illustrated in Figure 6.*

Theorem 3.6. (Multiple Barriers of M-SBM Merging to One, adapted from Mazzonetto [21]). *Before expressing the skewness parameter β for a general number of barriers n, we derive β for the first two simplest scenarios.*

If $n = 2$, $\beta_1, \beta_2 \in [-1, 1]$, $\mu \in \mathbb{R}$ and $x_2^{(n)} = x_1 + \frac{1}{n}$, $\forall n \in \mathbb{N}$. Let,

$$\beta := \frac{\beta_1 + \beta_2}{1 + \beta_1 \beta_2}.$$

Let us denote by $(X_t^{(n)})_t$ the (β_1, β_2)-SBM with drift μ, barriers $x_1, ..., x_n$, and denote by $(Y_t)_t$ the 1-SBM with drift μ, and barrier x_1. Let us assume $X_0^{(n)} = Y_0$, then $X^{(n)}$ converges to Y in the following sense,

$$\mathbb{E}\left[\sup_{s \in [0,t]} |X_s^{(m)} - Y_s|\right] \xrightarrow{m \to \infty} 0, \; \forall t \geqslant 0.$$

The same holds in the case of $n > 2$ barriers merging. In this case $(X_t^{(n)})_t$ is the $(\beta_1, ..., \beta_n)$-SBM with drift $\mu \in \mathbb{R}$, skewness parameters $\beta_1, ..., \beta_n \in [-1, 1]$ and barriers $x_1 \in \mathbb{R}$, $x_{j+1} := \frac{j}{n} + x_1$, $\forall j \in \{1, ..., n-1\}$.

The skewness parameter β of the limit 1-SBM is given by,

$$\beta := \frac{\displaystyle\prod_{j=1}^{n}(1 + \beta_j) - \prod_{j=1}^{n}(1 - \beta_j)}{\displaystyle\prod_{j=1}^{n}(1 + \beta_j) + \prod_{j=1}^{n}(1 - \beta_j)}. \tag{3.3}$$

If n is even,

$$\beta = \frac{\displaystyle\sum_{j=1}^{n}\beta_j + \sum_{j_1 < j_2 < j_3}\beta_{j_1}\beta_{j_2}\beta_{j_3} + ... + \sum_{j_1 < ... < j_{n-1}}\beta_{j_1}...\beta_{j_{n-1}}}{1 + \displaystyle\sum_{j_1 < j_2}\beta_{j_1}\beta_{j_2} + \sum_{j_1 < ... < j_4}\beta_{j_1}\beta_{j_2}\beta_{j_3}\beta_{j_4} + ... + \beta_1\beta_2...\beta_{j_n}}. \tag{3.4}$$

If n is odd,

$$\beta = \frac{\displaystyle\sum_{j=1}^{n}\beta_j + \sum_{j_1 < j_2 < j_3}\beta_{j_1}\beta_{j_2}\beta_{j_3} + ... + \beta_{j_1}...\beta_{j_n}}{1 + \displaystyle\sum_{j_1 < j_2}\beta_{j_1}\beta_{j_2} + \sum_{j_1 < ... < j_4}\beta_{j_1}\beta_{j_2}\beta_{j_3}\beta_{j_4} + ... + \sum_{j_1 < ... < j_{n-1}}\beta_1\beta_2...\beta_{j_{n-1}}}. \tag{3.5}$$

Proof. Refer to [21] and [15]. $\qquad\square$

The M-SBM framework also only considers one half-plane at a time, so that the transition density (or distribution) of the upper plane is assumed to be the same for the lower half plane, which is not always the case (except for BGCSP). We show below that whilst BGCSPs are a special case of M-SBMs, they have some unique properties that make them of particular interest among the larger class.

3.3. **Constructing BGC Stochastic Processes.** We can compliment Mazzonetto by condensing all possible local barrier combinations to the following four possible global barrier combinations that comprise a lower barrier α_j and an upper barrier α_k, as shown in Figure 7.
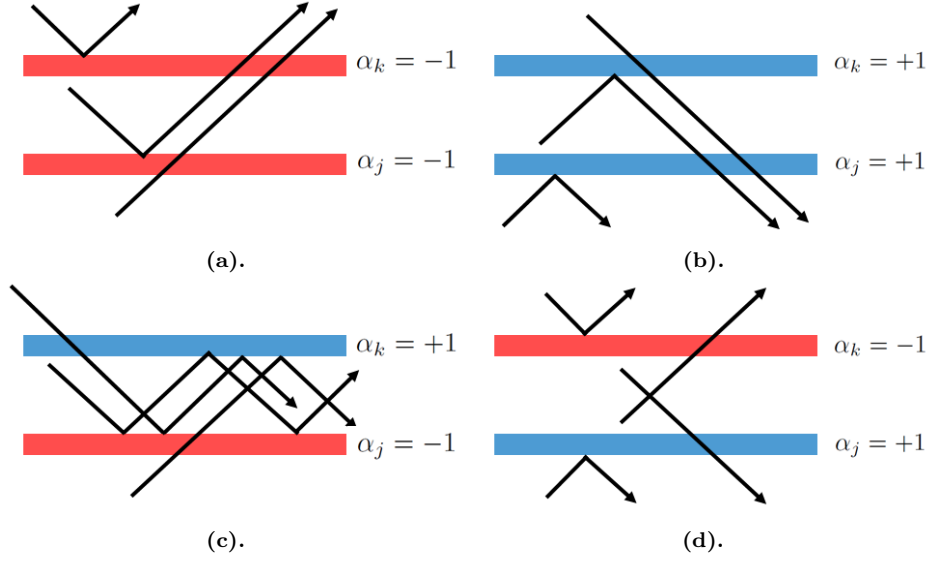

FIGURE 7. Generalised Barrier Combination Arguments

(a). All Itô diffusions will almost surely end up *above* the two negative fully reflective barriers.

(b). All Itô diffusions will almost surely end up *below* the two positive fully reflective barriers.

(c). All Itô diffusions will almost surely end up *within* the two fully reflective barriers.

(d). All Itô diffusions will almost surely end up *above or below (but not in between)* the two fully reflective barriers.

The diagrammatic summary of possible cases represented in Figure 7 is formally stated as Lemma 3.7 which is then used in Theorem 3.8. This Theorem formally expresses that the barriers of an M-SBM merge to a 1-SBM, to which the process converges.

Lemma 3.7. *If any $|\alpha_j| < 1$ for some $|\alpha_k| = 1$, or similarly for any $|\alpha_k| < 1$, then the barrier ± 1 will dominate the barrier $\neq \pm 1$, almost surely, as shown in Figure 7. Furthermore, if there are more than two fully reflective barriers, they will merge and effectively operate as one of the four possible combinations of Figure 7.*

Proof. We first assume that there exists only one reflective barrier $|\alpha_j| = 1$ and n semipermeable barriers $|\alpha_j| < 1$. We then consider the two SDEs;

$$
\begin{aligned}
X_t &= \mu_1\,dt + \sigma_1\,dW_t + \underbrace{\alpha_1\,dL_t^{\alpha_1}}_{|\alpha_i|=1} + \underbrace{\alpha_2\,dL_t^{\alpha_2} + ... + \alpha_n\,dL_t^{\alpha_n}}_{|\alpha_i|<1} \\
Y_t &= \mu_2\,dt + \sigma_2\,dW_t + \underbrace{\alpha_1\,dL_t^{\alpha_1}}_{|\alpha_i|=1}
\end{aligned}
\qquad , \qquad (3.6)
$$

where Y_t is an unconstrained Itô diffusion and X_t is a constrained Itô diffusion according to the above barrier constraints. Let $\delta = \sum_{i=1}^{n} \alpha_i$, so $\delta < 1$ or $\delta \geqslant 1$.

If $\delta < 1$, then α_i will dominate δ as it will vanish (i.e. $\delta \to 0$) such that,

$$
\sup_{t \to \infty} \left\{ |X_t| - |Y_t| \right\} = 0.
$$

If $\delta \geqslant 1$, then δ will dominate α_1 and merge (i.e. $\alpha_1 \to \delta$) such that,

$$
\sup_{t \to \infty} \left\{ |X_t| - |Y_t| \right\} = X_t.
$$

Next, assume that there exist two fully reflective barriers $|\alpha_j| = 1$, $|\alpha_k| = 1$ and n semipermeable barriers $|\alpha_i| < 1$. (3.6) now equates to,

$$
\begin{aligned}
X_t &= \mu_1\,dt + \sigma_1\,dW_t + \underbrace{\alpha_1\,dL_t^{\alpha_1}}_{|\alpha_i|=1} + \underbrace{\alpha_2\,dL_t^{\alpha_2} + ... + \alpha_n\,dL_t^{\alpha_n}}_{|\alpha_j|=1,\ |\alpha_k|=1} \\
&\quad + \underbrace{\alpha_1\,dL_t^{\alpha_1}}_{|\alpha_i|=1} + \underbrace{\alpha_2\,dL_t^{\alpha_2} + ... + \alpha_n\,dL_t^{\alpha_n}}_{\delta=|\alpha_i|<1} \\
Y_t &= \mu_2\,dt + \sigma_2\,dW_t + \underbrace{\alpha_1\,dL_t^{\alpha_1}}_{\delta=|\alpha_i|<1}
\end{aligned}
\qquad . \qquad (3.7)
$$

If $\delta < 1$, then α_j and (or) α_k will dominate δ and as it will vanish (i.e. $\delta \to 0$) and if $\delta \geqslant 1$, then δ will dominate α_j and (or) α_k hence merge to α_j and α_k, such that $\sup_{t \to \infty} \left\{ |X_t| - |Y_t| \right\} = 0$ and $\sup_{t \to \infty} \left\{ |X_t| - |Y_t| \right\} = X_t$, respectively.

Finally, if there are more than $N \geqslant 3$ fully reflective barriers $|\alpha_i| = 1$ and n semipermeable barriers, then the new barriers will effectively be a linear combination of any two possible combinations in Figure 7, depending on how the fully reflective barriers of N are defined, completing the proof for all scenarios. $\qquad \square$

To contrast Figure 4 for two reflective constant barriers, for BGCSP we have two hidden reflective barriers which also constrain the interior between the boundaries, as shown in Figure 8, where (a) shows the multiple barriers in $\mathbb{R}^2$, and (b) shows how the multiple barriers are projected from $\mathbb{R}^3$.

Leveraging the work of Ramirez [26], we partition X into countably infinite intervals $I_k = (x_k, x_{k+1})$, $\forall k \in \mathbb{R}$ forming the sequence $\{I_{-\infty}, ..., I_{-1}, I_1, ..., I_\infty\}$ such that the standard conditions are met; $I_k \bigcap I_{k+1} = \varnothing$ $\forall k \in \mathbb{R}$, $\varnothing \notin X$ and $\bigcup_{k=-\infty}^{\infty} I_k = X$. We wish to shrink the size of each interval $|I_k| = |x_{k+1} - x_k|$ to zero as we apply more and more intervals, where $\lim_{k \to \infty} |x_{k+1} - x_k| \to 0$ and $\int_{-\infty}^{\infty} I_k\,dk < \infty$. This is because we wish to constrain the Itô diffusion by the BGC function $\Psi(X_t, t) \in \mathbb{R}$.

(a). Barrier in $\mathbb{R}^2$ - Contour plot   (b). Barrier in $\mathbb{R}^3$- Contour & surface plot
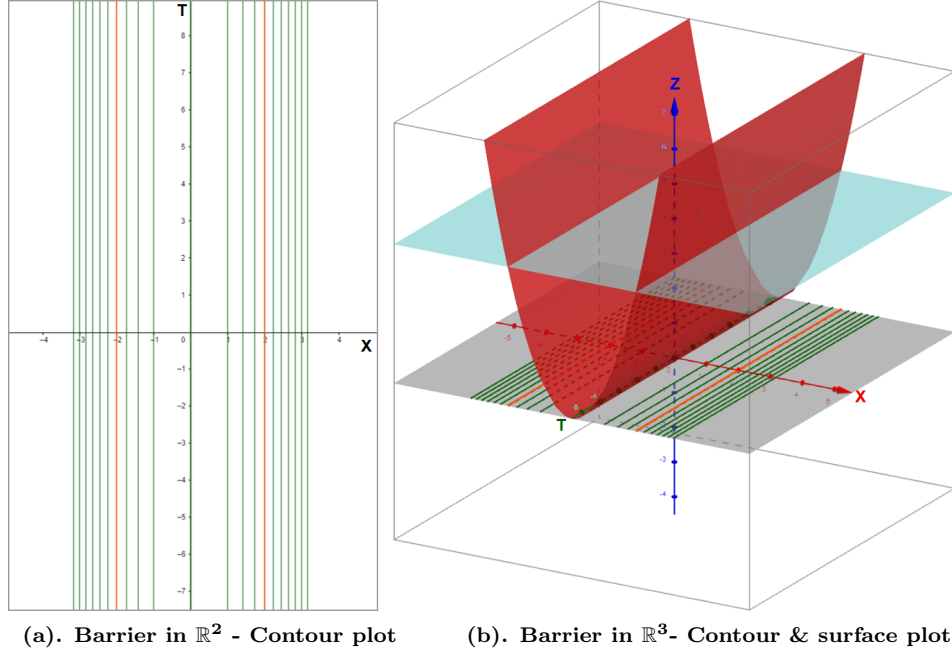
FIGURE 8. Diffusion Between Two BGC Reflective Barriers

As the light blue plane $z = k$ for $k \in \mathbb{R}_+$ descends to the origin, the green (and orange) contour lines of the BGC reflective barriers change in accordance with the red BGC function $\Psi(X_t, t)$.

In terms of BGC stochastic processes, we effectively have a $(\beta_{-n}, ..., \beta_{-1}, \beta_1, ..., \beta_n)$-SBM and will express it as,

$$
\begin{cases}
dX_t & = \quad \mu \, dt + \sigma \, dW_t + \underbrace{\underbrace{\sum_{j=-n}^{-1} \beta_j \, dL_t^{x_j}}_{<0} + \underbrace{\sum_{j=1}^{n} \beta_j \, dL_t^{x_j}}_{>0}}_{\Psi(X_t, t)} \\
X_0 & = \quad 0 \\
\mathcal{E} & = \quad \{\mu, \sigma, (\beta_{-n}, ..., \beta_{-1}, \beta_1, ..., \beta_n)\} \in \mathbb{R} \\
L_t^{x_j} & = \quad \int_0^t \mathbb{1}_{\{X_s = z_j\}} \, dL_s^{x_j}, \; j \in \{-n, ..., -1, 1, ..., n\}
\end{cases}
, \qquad (3.8)
$$

as illustrated in Figure 9.

Theorem 3.8. *(Skewness Parameter of BGC Stochastic Processes). Let us denote by $(X_t^{(n)})_t$ the $(\beta_{-n}, ..., \beta_n)$-SBM with drift μ and barriers $x_{-n}, ..., x_n$, and denote by $(Y_t)_t$ the 2-SBM (i.e. β_1, β_2-SMB) with drift μ, diffusion σ and barrier x_1. Let us assume $X_0^{(n)} = Y_0$, then $X^{(n)}$ converges to Y in the following sense,*
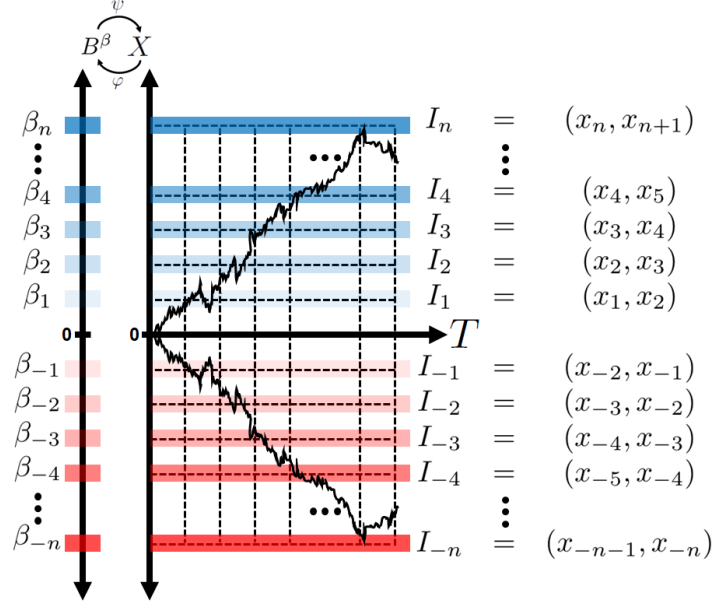
FIGURE 9. Constructing BGC Stochastic Processes from M-SBM Framework

As the Itô process reaches further and further intervals I_k from the origin, the intervals' permeability decreases and is scaled by β_k. The less permeable the interval becomes, the more it operates as a reflective barrier. Eventually, there exists an interval that for the given Itô diffusion is effectively fully reflective, forming the hidden barrier of BGC stochastic processes.

$$\lim_{n \to \infty} \left\{ \mathbb{E}\left[\sup_{s \in [0,t]} |X_s^{(n)} - Y_s| \right] \right\} = 0, \ \forall t \in [0, T].$$

The same holds in the case of $n > 2$ barriers merging. In this case $(X_t^{(n)})_t$ is the $(\beta_{-n}, ..., \beta_n)$-SBM with drift $\mu \in \mathbb{R}$, diffusion $\sigma \in \mathbb{R}$, skewness parameters $\beta_{-n}, ..., \beta_n \in [-1, 1]$ and barrier $x_1 \in \mathbb{R}$, $x_{j+1} := \frac{j}{n} + x_1$, $\forall j \in \{1, ..., n-1\}$. Then $\beta = 0$.

Proof. In contrast to the skewness parameter of the limit 1-SBM in (3.3), the corresponding skewness parameter of the limit 2-SBM for BGCSP is given by (3.9),

$$\beta \ := \ \underbrace{\frac{\prod_{j=1}^{n}(1+\beta_j) - \prod_{j=1}^{n}(1-\beta_j)}{\prod_{j=1}^{n}(1+\beta_j) + \prod_{j=1}^{n}(1-\beta_j)}}_{>\mathbf{0}} + \underbrace{\frac{\prod_{j=-1}^{-n}(1+\beta_j) - \prod_{j=-1}^{-n}(1-\beta_j)}{\prod_{j=-1}^{-n}(1+\beta_j) + \prod_{j=-1}^{-n}(1-\beta_j)}}_{<\mathbf{0}}$$

$$= \ \frac{\left[\prod_{j=1}^{n}(1+\beta_j) - \prod_{j=1}^{n}(1-\beta_j)\right]\left[\prod_{j=-1}^{-n}(1+\beta_j) + \prod_{j=-1}^{-n}(1-\beta_j)\right] + \left[\prod_{j=1}^{n}(1+\beta_j) + \prod_{j=1}^{n}(1-\beta_j)\right]\left[\prod_{j=-1}^{-n}(1+\beta_j) - \prod_{j=-1}^{-n}(1-\beta_j)\right]}{\left[\prod_{j=1}^{n}(1+\beta_j) + \prod_{j=1}^{n}(1-\beta_j)\right]\left[\prod_{j=-1}^{-n}(1+\beta_j) + \prod_{j=-1}^{-n}(1-\beta_j)\right]}$$

$$= \ \frac{\left[\prod_{j=1}^{n}(1+\beta_j)\prod_{j=-1}^{-n}(1+\beta_j) + \prod_{j=1}^{n}(1+\beta_j)\prod_{j=-1}^{-n}(1-\beta_j) - \prod_{j=1}^{n}(1-\beta_j)\prod_{j=-1}^{-n}(1+\beta_j) - \prod_{j=1}^{n}(1-\beta_j)\prod_{j=-1}^{-n}(1-\beta_j)\right]}{\left[\prod_{j=1}^{n}(1+\beta_j)\prod_{j=-1}^{-n}(1+\beta_j) + \prod_{j=1}^{n}(1+\beta_j)\prod_{j=-1}^{-n}(1-\beta_j) + \prod_{j=1}^{n}(1-\beta_j)\prod_{j=-1}^{-n}(1+\beta_j) + \prod_{j=1}^{n}(1-\beta_j)\prod_{j=-1}^{-n}(1-\beta_j)\right]}$$
$$+ \ \frac{\left[\prod_{j=1}^{n}(1+\beta_j)\prod_{j=-1}^{-n}(1+\beta_j) - \prod_{j=1}^{n}(1+\beta_j)\prod_{j=-1}^{-n}(1-\beta_j) + \prod_{j=1}^{n}(1-\beta_j)\prod_{j=-1}^{-n}(1+\beta_j) - \prod_{j=1}^{n}(1-\beta_j)\prod_{j=-1}^{-n}(1-\beta_j)\right]}{\left[\prod_{j=1}^{n}(1+\beta_j)\prod_{j=-1}^{-n}(1+\beta_j) + \prod_{j=1}^{n}(1+\beta_j)\prod_{j=-1}^{-n}(1-\beta_j) + \prod_{j=1}^{n}(1-\beta_j)\prod_{j=-1}^{-n}(1+\beta_j) + \prod_{j=1}^{n}(1-\beta_j)\prod_{j=-1}^{-n}(1-\beta_j)\right]}.$$

(3.9)

Noting that due to the symmetry of BGCSP about the origin,

$$\prod_{j=-1}^{-n}(1-\beta_j) = \prod_{j=1}^{n}(1+\beta_j), \quad \prod_{j=-1}^{-n}(1+\beta_j) = \prod_{j=1}^{n}(1-\beta_j),$$

which allows the $\prod_{j=1}^{n}(1+\beta_j)$ terms to factor out in (3.9) giving,

$$\beta \ = \ \frac{\prod_{j=1}^{n}(1+\beta_j)\left[\prod_{j=-1}^{-n}(1+\beta_j) + \prod_{j=-1}^{-n}(1-\beta_j) - \prod_{j=1}^{n}(1-\beta_j) - \prod_{j=1}^{n}(1-\beta_j)\prod_{j=-1}^{-n}(1+\beta_j)\bigg/\prod_{j=1}^{n}(1+\beta_j)\right]}{\prod_{j=1}^{n}(1+\beta_j)\left[\prod_{j=-1}^{-n}(1+\beta_j) + \prod_{j=-1}^{-n}(1-\beta_j) + \prod_{j=1}^{n}(1-\beta_j) + \prod_{j=1}^{n}(1-\beta_j)\prod_{j=-1}^{-n}(1+\beta_j)\bigg/\prod_{j=1}^{n}(1+\beta_j)\right]}$$
$$+ \ \frac{\prod_{j=1}^{n}(1+\beta_j)\left[\prod_{j=-1}^{-n}(1+\beta_j) - \prod_{j=-1}^{-n}(1-\beta_j) - \prod_{j=1}^{n}(1-\beta_j) + \prod_{j=1}^{n}(1-\beta_j)\prod_{j=-1}^{-n}(1+\beta_j)\bigg/\prod_{j=1}^{n}(1+\beta_j)\right]}{\prod_{j=1}^{n}(1+\beta_j)\left[\prod_{j=-1}^{-n}(1+\beta_j) + \prod_{j=-1}^{-n}(1-\beta_j) + \prod_{j=1}^{n}(1-\beta_j) + \prod_{j=1}^{n}(1-\beta_j)\prod_{j=-1}^{-n}(1+\beta_j)\bigg/\prod_{j=1}^{n}(1+\beta_j)\right]}$$

which expands to,

$$\beta \;=\; \frac{\left[\displaystyle\prod_{j=-1}^{-n}(1-\beta_j) - \left(\prod_{j=1}^{n}(1-\beta_j)\right)^2 \Big/ \prod_{j=1}^{n}(1+\beta_j) \right]}{\left[\displaystyle\prod_{j=-1}^{-n}(1+\beta_j) + \prod_{j=-1}^{-n}(1-\beta_j) + \prod_{j=1}^{n}(1-\beta_j) + \left(\prod_{j=1}^{n}(1-\beta_j)\right)^2 \Big/ \prod_{j=1}^{n}(1+\beta_j) \right]}$$

$$+ \frac{\left[-\displaystyle\prod_{j=-1}^{-n}(1-\beta_j) + \left(\prod_{j=1}^{n}(1-\beta_j)\right)^2 \Big/ \prod_{j=1}^{n}(1+\beta_j) \right]}{\left[\displaystyle\prod_{j=-1}^{-n}(1+\beta_j) + \prod_{j=-1}^{-n}(1-\beta_j) + \prod_{j=1}^{n}(1-\beta_j) + \left(\prod_{j=1}^{n}(1-\beta_j)\right)^2 \Big/ \prod_{j=1}^{n}(1+\beta_j) \right]}. \tag{3.10}$$

It is clear that the numerator equates to 0 and so $\beta = 0$, completing the proof. $\quad\square$

Remark 3.9. *Due to the bi-directionality of BGC stochastic processes, then n in (3.4) is always even, so $\beta = 0$. From Portenko [25], if $|x_i| \leqslant 1$, then $|\sum_{i=1}^{n} \alpha_i| \geqslant 1$ is of special interest. With BGCSP, $\alpha_{-n} + \alpha_n = 0$, $\alpha_{-n+1} + \alpha_{n-1} = 0$,...,$\alpha_{-1} + \alpha_1 = 0$ due to their symmetry about the origin, hence $|\sum_{i=1}^{n} \alpha_i| = 0$ as well.*

Theorem 3.10. *(Cylindrical BGCSPs are 2-SBMs). For a complete filtered probability space $(\Omega, \mathcal{F}, \{\mathcal{F}\}_{t\geqslant0}, \mathbb{P})$ and a BGC function $\Psi(y) : \mathbb{R} \to \mathbb{R}$, $\forall y \in \mathbb{R}$, then the corresponding BGC Itô diffusion is defined as follows,*

$$dY_t = f(Y_t, t)\, dt + g(Y_t, t)\, dW_t - \underbrace{\mathrm{sgn}[Y_t]\Psi(Y_t, t)}_{BGC}, \tag{3.11}$$

where $f(Y_t, t)$ is the drift coefficient, $g(Y_t, t)$ is the diffusion coefficient, $\mathrm{sgn}[x]$ is the usual sign function, $f(Y_t, t)$, $g(Y_t, t)$, $\Psi(Y_t, t)$ are convex functions and the 2-SBM is defined by,

$$\begin{cases} dX_t &=& \mu\, dt + \sigma\, dW_t + \underbrace{\beta_{-1}\, dL_t^{x_{-1}}}_{<0} + \underbrace{\beta_1\, dL_t^{x_1}}_{>0} \\[2mm] X_0 &=& 0,\; \mathcal{E}\Big(\mu, \sigma, (\beta_{-1}, \beta_1)\Big) \\[1mm] L_t^{x_j} &=& \int_0^t \mathbb{1}_{\{X_s = z_j\}}\, dL_s^{x_j},\; j \in \{-1, 1\} \end{cases}, \tag{3.12}$$

then, $Y_t \to X_t$ almost surely.

Proof. It is conceivable that under general non-constant $f(X_t, t)$ and $g(X_t, t)$ and some generalized BGC function $\Psi'(f(X_t, t), g(X_t, t), X_t, t)$ that $\Psi'(x)$ could modulate X_t such that it is bounded above and below by a constant barrier at a and b, respectively, where $b = -a$. For this theorem, we are required to prove that constant over time (i.e. cylindrical) BGC functions $\Psi(X_t, t)$ will converge almost surely to a 2-SBM. We know from at least Krykun [14] that if $|\alpha_i| \leqslant 1$, $i \in \{1, ..., n\}$, there exists a strong solution to (3.12). Since the BGC functions $\Psi(X_t, t) \in \mathbb{R}$ are convex, there exists some value κ for both a hidden lower barrier $\mathfrak{B}_L$ and a hidden upper barrier $\mathfrak{B}_L$ that are induced by $\Psi(X_t, t)$. For BGCSP, there is no fully reflective barrier defined in advance as there is with M-SBM. However, there are still two fully reflective barriers in BGCSP because the BGC term $\Psi(X_t, t)$ will enable the constrained Itô process Y_t to eventually be overtaken by the underlying unconstrained Itô process X_t such that $|X_s^{(n)}| \geqslant |Y_s|$ giving,

$$\mathfrak{B}_U = \kappa \text{ for } \lim_{n \uparrow \kappa} \left\{ \mathbb{E}\left(\sup_{s \in [0,t]} \left| |X_s^{(n)}| - |Y_s| \right| \right) \right\} = 0, \tag{3.13}$$

$$\mathfrak{B}_L = -\kappa \text{ for } \lim_{n \downarrow -\kappa} \left\{ \mathbb{E}\left(\sup_{s \in [0,t]} \left| |X_s^{(n)}| - |Y_s| \right| \right) \right\} = 0. \tag{3.14}$$

For this to be true, it must be shown that $\kappa > 0$ exists. We create a small neighborhood $\mathcal{N}$ about the initial point x_0 of radius $\epsilon \in \mathbb{R}_+$ such that $\mathcal{N}(x_0) = (x_0 - \epsilon, x_0 + \epsilon)$. As $\epsilon \to +\infty$, $\mathfrak{B}_L$ and $\mathfrak{B}_U$ will eventually lie in $\mathcal{N}(x_0)$.

If $x_0 > 0$, then $\sup\{\mathcal{N}(x_0)\} = x_0 + \min(\epsilon)$ such that $\mathfrak{B}_U = \sup\{\mathcal{N}(x_0)\} = \kappa$.
If $x_0 = 0$, then $\sup\{\mathcal{N}(x_0)\} = \inf\{\mathcal{N}(x_0)\}$ such that $\mathfrak{B}_L = -\mathfrak{B}_U = |\mathfrak{B}_U| = \kappa$.
If $x_0 < 0$, then $\inf\{\mathcal{N}(x_0)\} = x_0 - \min(\epsilon)$ such that $\mathfrak{B}_L = \inf\{\mathcal{N}(x_0)\} = -\kappa$.

Hence κ exists and its value is $\kappa = f(\Psi(X_t, t), X_t, t, \mu, \sigma)$ for some function $f : \mathbb{R} \to \mathbb{R}$. Having found κ, we know that the reflectiveness at $\pm\kappa$, i.e. $|\beta_\kappa| = 1$, $|\beta_{-\kappa}| = 1$ and before $\pm\kappa$, i.e. $|\beta_i| < 1$, $|\beta_{-i}| < 1$. Hence, $\beta_{-\kappa}, ..., \beta_{-1}, \beta_1, ..., \beta_\kappa$ for X_t must be scaled for Y_t by $\Psi(X_t, t)$ and since $\Psi(X_t, t)$ is strictly convex and symmetrical about the origin, then the ordering is preserved,

$$\frac{\beta_{-\kappa}}{\Psi(\kappa, t)} < ... < \frac{\beta_{-1}}{\Psi(\kappa, t)} < \frac{\beta_1}{\Psi(\kappa, t)} < ... < \frac{\beta_\kappa}{\Psi(\kappa, t)}. \tag{3.15}$$

(3.15) ensures that a strong solution to BGCSP exists within a 2-SBM framework, completing the proof. $\qquad\square$

So far, our formulations of BGC functions have been expressed in the general form $\Psi(X_t, t)$, but we have considered BGC barriers induced by time-independent convex surfaces which can be specified by just $\Psi(X_t)$, hence M-SBM is related to BGCSPs with $\Psi(X_t)$. However, since the barriers have been specified to be able to change not only under space (distance) but over time as well, we demonstrate this additional complexity of BGCSPs in Figure 10.
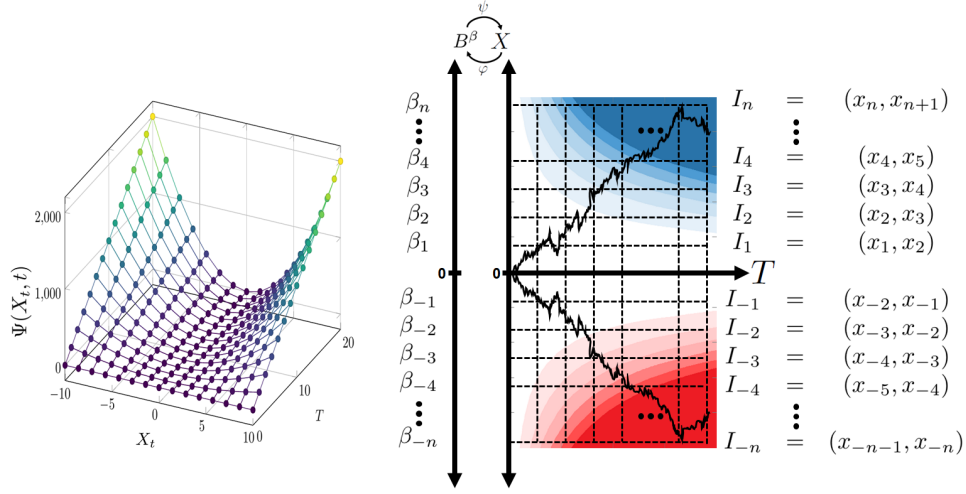
FIGURE 10. Example BGC Function $\Psi(X_t, t)$ Constraining BGC-SPs over Space and Time, more so than in M-SBM

BGCSPs are more expansive than M-SBMs (compare with Figure 6) in the sense that the barriers can change over time, hence $\Psi(X_t, t)$ rather than the simpler $\Psi(X_t)$, which is related to M-SBM. The mesh plot on the left induces or dictates how the BGCSP on the right is constrained, showing that the M-SBM doesn't cover such time-dependent constraints.

4. RESULTS AND DISCUSSION

In the following simulations, the underlying unconstrained Itô diffusions have drift $\mu = 0$ and diffusion $\sigma = 1$, resulting in just the Wiener process. This is so that the subsequent impact of BGC can be easily compared. Despite this, we still refer to these as the more general Itô diffusions because these parameters can be modified for one's specific requirements.

To validate the existing M-SBM research and to support our comparison of BGCSP with M-SBM, we develop Algorithm 1 which is used to progressively introduce additional reflective barriers. In the subsequent series of simulations, we introduce 2, 4, 8, 16 and finally 32 semipermeable barriers, with increasing reflectiveness (i.e. decreasing permeability) the further the Itô diffusion is from the origin, which are simulated via Algorithm 1.

The simplest application of Algorithm 1 is shown for two fully reflective barriers in Figure 11.

**Algorithm 1:** Approximating BGC Stochastic Processes via Successive Reflective Barriers

```
 1  # Pseudocode based on R
 2  INPUT:
 3  μ = drift, σ = diffusion, i = simulation index, s= # simulations = 10,000, t =
      time steps = 1001, j = time index, Print_Simulations = TRUE
 4  OUTPUT:
 5  ID_value ← matrix(0 : 0, nrow = TimeSteps, ncol = Simulations)
 6  T_1000 ← matrix(0 : 0, nrow = Simulations, ncol = 1)
 7  for (i=1:s) do
 8      for (j=1:t) do
 9          if (t==1) then
10              │   ID_value[t, i] ← 0
11          else
12                  dt = (t/TimeSteps)
13                  ID_value[t, i] ← (μ * dt + σ * rnorm(1))
14                  Sum_ID_value ← sum(ID_value[, i])
15
16                  # UPPER BARRIERS================================
17                  if ((Sum_ID_value > 0) && (Sum_ID_value <= UpperBarrier_01)) then
18                  │   Do nothing;
19                  else if ((Sum_ID_value > UpperBarrier_01) && (Sum_ID_value <=
                      UpperBarrier_02)) then
20                  │   ID_value[t, i] ← (ID_value[t, i] − abs(ID_value[t, i] * ID_value[t, i])/100)
21                  else if (Sum_ID_value > UpperBarrier_16) then
22                  │   ID_value[t, i] ← (−abs(ID_value[t, i]))
23                  else
24                  │   ID_value[t, i] ← ID_value[t, i]
25                  end if
26
27                  # LOWER BARRIERS================================
28                  if ((Sum_ID_value < 0) && (Sum_ID_value >= LowerBarrier_01)) then
29                  │   Do nothing;
30                  else if (Sum_ID_value < LowerBarrier_16) then
31                  │   ID_value[t, i] ← (abs(ID_value[t, i]))
32                  else
33                  │   ID_value[t, i] ← ID_value[t, i]
34                  end if
35          end if
36          if (Print_Simulations==TRUE) then
37              if (i==1) then
38              │   plot(T, cumsum(ID_value[, i]), type = "l", ylim = c(yMax, yMin))
39              else
40              │   lines(T, cumsum(ID_value[, i]), type = "l", ylim = c(yMax, yMin))
41              end if
42          end if
43      end for
44      T_1000[i] < −sum(ID_value[, i])
45  end for
```
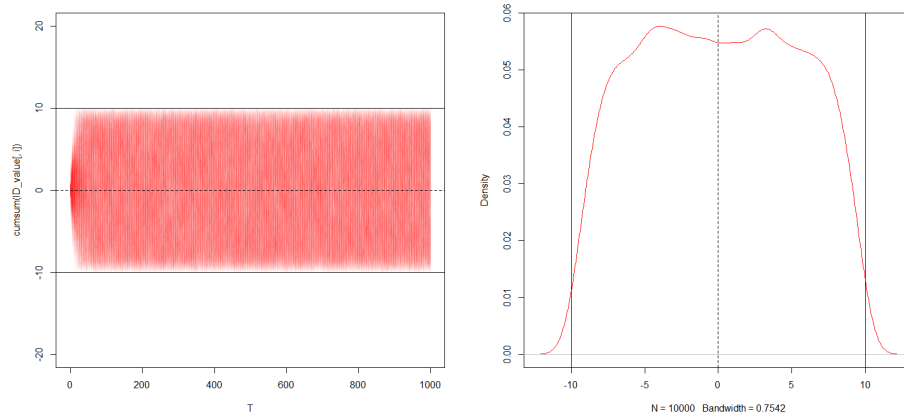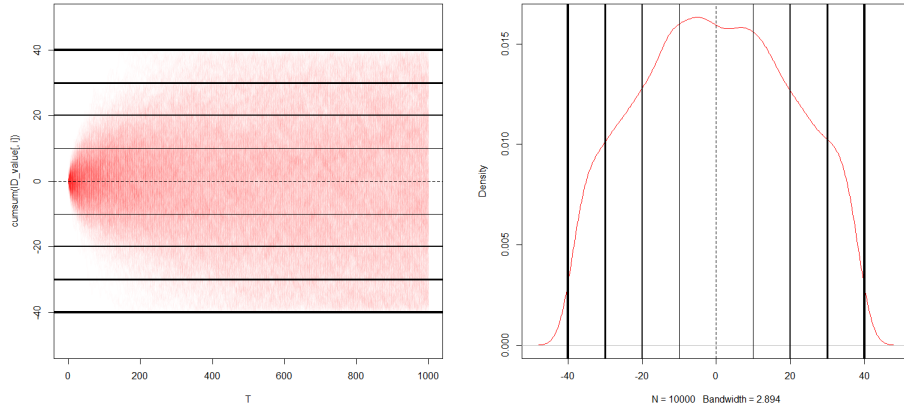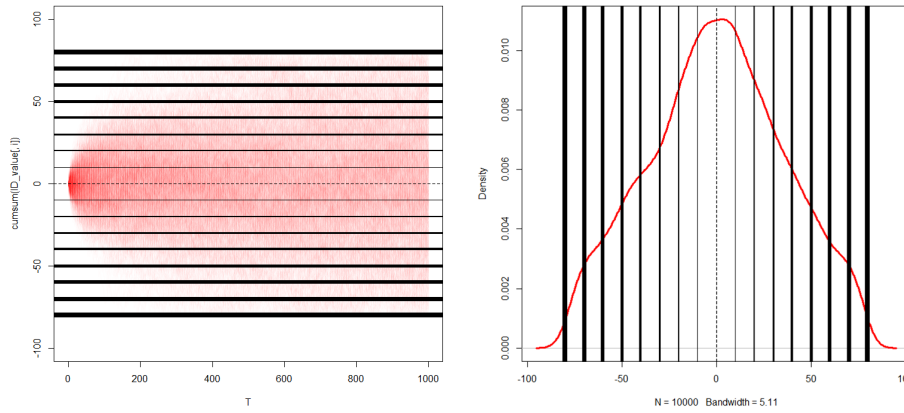

(a). 1,000 Simulations,   (b). 10,000 Simulation Density

FIGURE 11. 10,000 Simulations of 1,000 Step 1-Dimensional Itô Diffusions With 2 Reflective Barriers

Figure 11 has 2 fully reflective barriers at ± 10 generated using Algorithm 1. This was then increased to 4 barriers (2 fully reflective and 2 semipermeable) as shown in Figure 12.
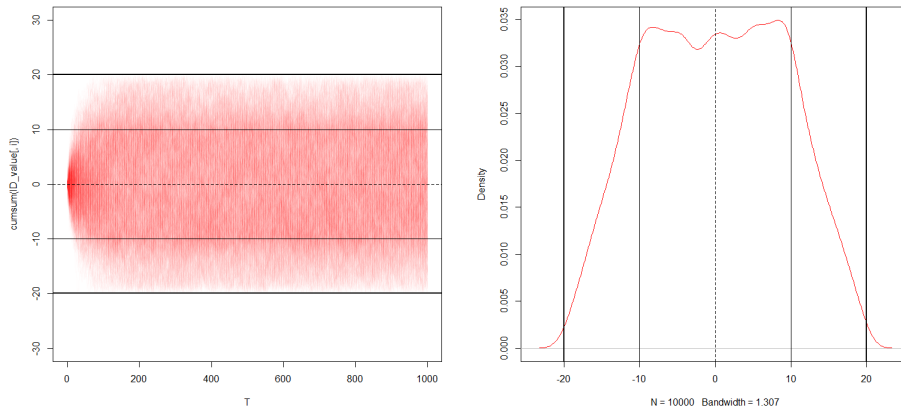
(a). 1,000 Simulations,   (b). 10,000 Simulation Density
FIGURE 12. 10,000 Simulations of 1,000 Step 1-Dimensional Itô Diffusions With 4 Reflective Barriers

In Figure 12, we make the barriers at ± 20 fully reflective and the barriers at ± 10 now to be semipermeable. Although it may not yet be apparent due to the thickness of the drawn barriers, we have and will continue to increase the thickness of the barriers to highlight the increasing reflectiveness (and decreasing semipermeability) the further the Itô diffusions are from the origin. The total number of barriers was doubled again to result in 8 barriers (2 fully reflective and 6 semipermeable), as shown in Figure 13.
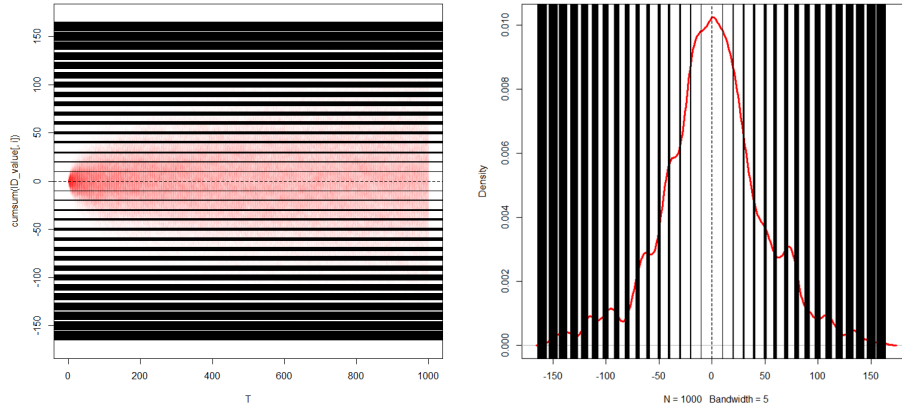
(a). 1,000 Simulations,   (b). 10,000 Simulation Density
FIGURE 13. 10,000 Simulations of 1,000 Step 1-Dimensional Itô
Diffusions With 8 Reflective Barriers

In Figure 13(b), we start to notice a corrugation or 'crinkling' of the density due
to 2 fully reflective barriers and 6 semipermeable barriers. This was doubled again
to 16 barriers (2 fully reflective and 14 semipermeable), as shown in Figure 14.

(a). 1,000 Simulations,   (b). 10,000 Simulation Density
FIGURE 14. 10,000 Simulations of 1,000 Step 1-Dimensional Itô
Diffusions With 16 Reflective Barriers

In Figure 14(b), we notice that the corrugation effect has become more pronounced
due to another doubling of the number of barriers. This was doubled again to 32
barriers (2 fully reflective and 30 semipermeable), as shown in Figure 15.

(a). 1,000 Simulations,   (b). 10,000 Simulation Density
FIGURE 15. 10,000 Simulations of 1,000 Step 1-Dimensional Itô
Diffusions With 32 Reflective Barriers

Finally, in Figure 15(b), we notice the most amount of the corrugation effect due
to yet another doubling of the number of semipermeable barriers. Due to the
importance of this density as a sufficient approximation of BGC densities, we plot
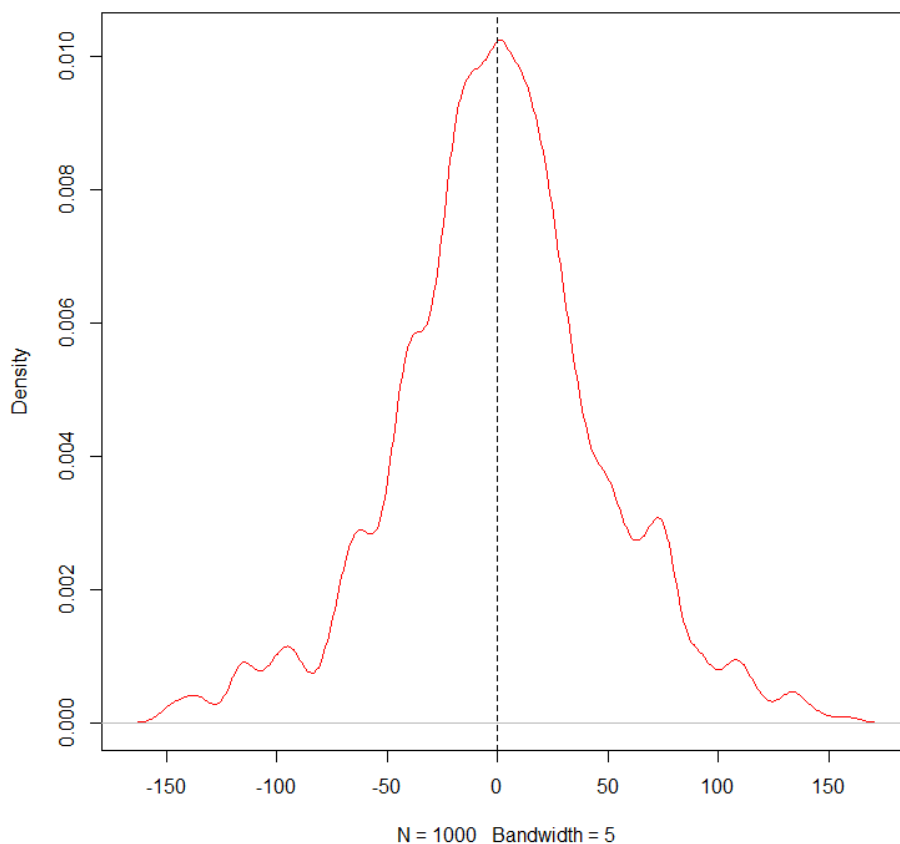the density again in Figure 16 without the barriers depicted and slightly larger.

FIGURE 16. Typical Density of BGC Itô Diffusions Approximated by 10,000 Simulations of 1,000 Step 1-Dimensional Itô Diffusions With 32 Reflective Barriers

Figure 16 shows that after 32 barriers, we effectively arrive at the typical density of BGC Itô diffusions, which have an infinite number of increasingly reflective barriers, with just 2 fully reflective hidden barriers. If we take the limit of this numerical approximation process, the number of such barriers n would approach infinitely many barriers, of smaller and smaller size and hence smaller constraining contribution. These approximation barriers are thus replaced by the main BGC function itself, $\Psi(X_t, t) = (\frac{X_t}{10})^2$, as shown in Figure 17, where the algorithm for BGCSP was stated in [32].
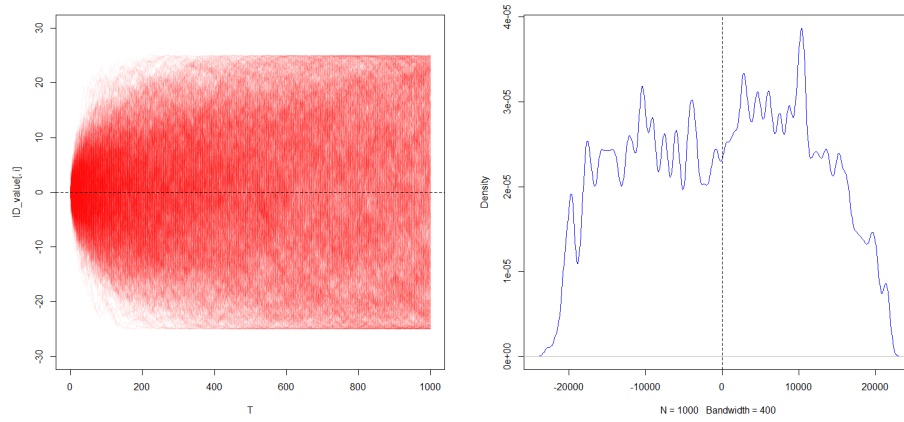
(a). 1,000 Simulations,   (b). 10,000 Simulation Density

FIGURE 17. 10,000 Simulations of 1,000 Step BGC 1-Dimensional
Itô Diffusions

From Figure 17, we see the typical characteristics of BGCSPs; 1). a certain amount
of discretization or banding at various local times, 2). the emergence of two hidden
reflective barriers that are not known exactly in advance and can only be estimated,
3). the density is 'corrugated' or 'rough'.

The random component of the Itô diffusions, i.e. the dW_t term is sampled from a
standard normal distribution that is then constrained by BGCSP. The density of
Figure 17(b) has no discontinuities. However, if we sample the path increments from
a discrete binary (i.e. binomial) random distribution, we obtain a random walk that
is then constrained by BGCSP. When a histogram is derived for the corresponding
simulated data rather than fitting a density through the distribution, we obtain
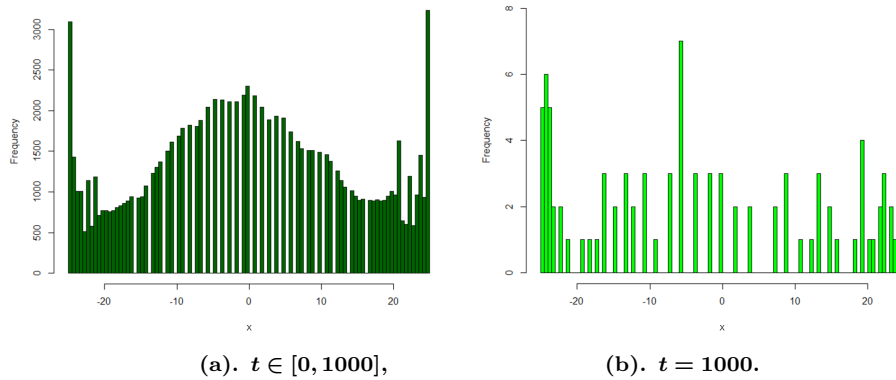Figure 18, which shows the discontinuities, also evident in [33].

(a). $t \in [0, 1000]$,   (b). $t = 1000$.

FIGURE 18. Histogram of 10,000 Simulations of 1,000 Step BGC
1-Dimensional Itô Diffusions Showing Discretization or Banding,
for Sampling dW_t from a Binomial Distribution

**Note that this is not a density plot as we do not want any Kernal density estimation
(KDE) to approximate the distribution. Increasing the bin size would similarly
approximate the histogram. The main point is that when we consider all points
along all paths in (a), we see gaps where the paths do not visit, or visit infrequently.
When we only detect the paths at the end of our timeframe in (b), we see many
more gaps and that the gaps are not as homogeneously dispersed as in (a).**

Figure 18 shows that 1). reflection occurs at the barriers as seen by the peaks
on either side of the distribution (more prominent in (a)), and 2). discretization
or banding occurs at prominent local times that are contracted together due to
the BGC function $\Psi(X_t, t)$. Figure 18(a) shows similar 'corrugation' as in the
continuous case in Figure 16. Figure 18(b) shows that at $t = T$, the BGC Itô
diffusion is less likely to be at the origin and more likely to be near the barrier(s).
To further demonstrate the characteristics of BGCSP, a detailed plot of 10,000
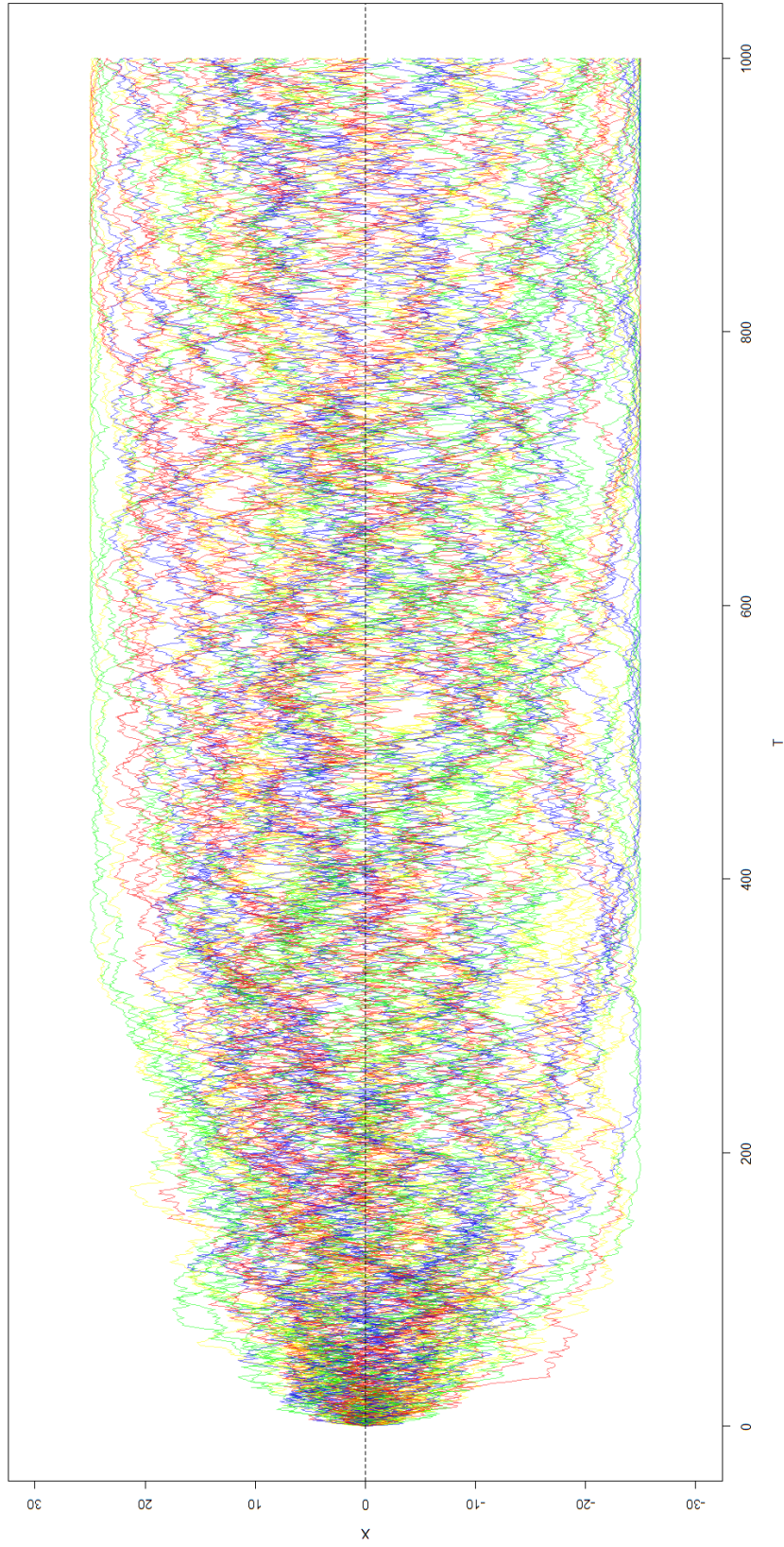simulations are shown in Figures 19 and 20.

FIGURE 19. 200 BGC Itô Diffusions Sampled from the Standard Normal Distribution

The hidden barriers emerge as the Itô diffusions reach their equilibrium point(s). The reflectiveness of $\Psi(X_t, t)$ induces the hidden barriers $\mathcal{B}_L$, $\mathcal{B}_U$ and they become more visible over time.
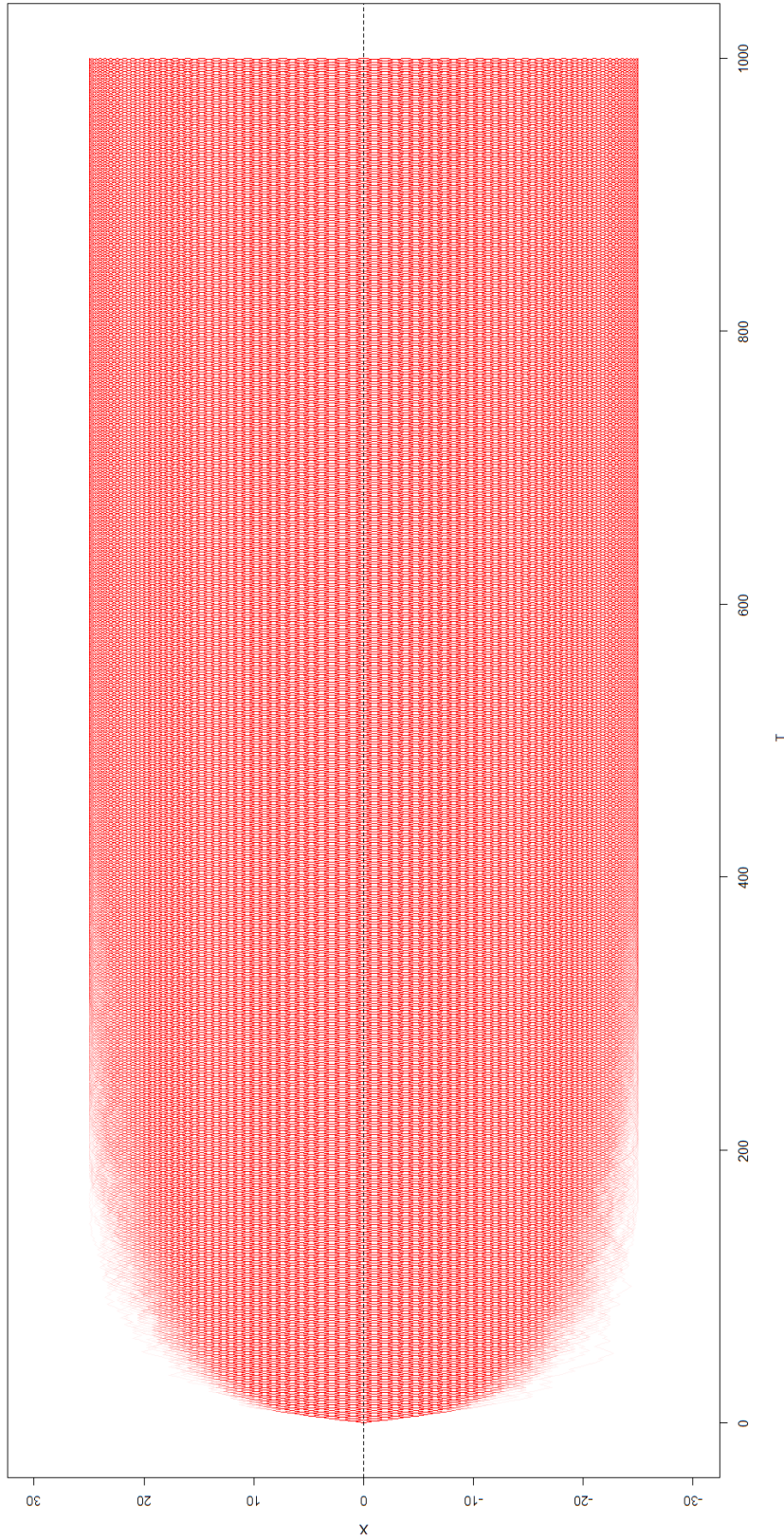
FIGURE 20. 1,000 BGC Itô Diffusions Sampled from the Standard Normal Distribution

Even with continuous dW_t, there are regions where the paths do not visit as often. This would be more noticeable as with our previous research [33], [32], if only the markers were used rather than the markers and the lines, as is the case in this plot. We notice a certain amount of banding in regions on either side of the origin. These regions become closer and closer together the further X is away from the origin. The use of opacity facilitates these regions to be more visible, otherwise, it would be a uniformly red rectangular region.

5. Conclusions

This paper has extended the previous theoretical research on BGCSP by comparing them to a type of multi-skew Brownian motion (M-SBM). This was achieved both theoretically by leveraging existing research, and heuristically by generating new simulations. Working within the M-SBM framework, we proved one Lemma and two Theorems for BGCSPs. This research provides a richer framework in which the semipermeable barriers are modulated in a non-constant manner over distance X, allowing for a new constraining regime that is more complex than the Ornstein-Uhlenbeck process (OUP) and yet still related to it. BGCSPs have applications in many fields requiring the constraining of the underlying stochastic process in a gradual manner where the two ultimate reflective barriers are not known in advance.

References

[1] Appuhamillage, T. and Sheldon, D. (2012). First passage time of skew brownian motion. *J. Appl. Probab.*, 49(3):685–696.

[2] Atar, R. and Budhiraja, A. (2015). On the multi-dimensional skew brownian motion. *Stochastic Process. Appl.*, 125(5):1911–1925.

[3] Ball, C. A. and Roma, A. (1998). Detecting mean reversion within reflecting barriers: application to the european exchange rate mechanism. *Applied Mathematical Finance*, 5(1):1–15.

[4] Bramson, M., Dai, J., and Harrison, J. (2010). Positive recurrence of reflecting brownian motion in three dimensions. *The Annals of Applied Probability*, 20(2):753–83.

[5] Budhiraja, A. and Dupuis, P. (2003). Large deviations for the empirical measures of reflecting brownian motion and related constrained processes in r+. *Electronic Journal of Prob.*, 8.

[6] Dereudre, D., Mazzonetto, S., and Roelly, S. (2015). An explicit representation of the transition densities of the skew brownian motion with drift and two semipermeable barriers. *arXiv preprint arXiv:1509.02846.*

[7] Dua, S., Khadilkar, S., and Sen, K. (1976). A modified random walk in the presence of partially reflecting barriers. *J. Appl. Prob.*, 13:169–175.

[8] Gairat, A. and Shcherbakov, V. (2017). Density of skew brownian motion and its functionals with application in finance. *Mathematical Finance*, 27(4):1069–1088.

[9] Gupta, H. (1966). Random walk in the presence of a multiple function barrier. *Journ. Math. Sci.*, 1:18–29.

[10] Harrison, J. and Shepp, L. (1981). On skew brownian motion. *Ann. Probab.*, 9(2):309–313.

[11] Harrison, M. (1986). *Brownian Motion and Stochastic Flow Systems.* John Wiley & Sons.

[12] Hu, Q., Wang, Y., and Yang, X. (2012). The hitting time density for a reflected brownian motion. *Computational Economics*, 40(1):1–18.

[13] Itô, K. and McKean, H. (1965). *Diffusion Processes and Their Sample Paths.* Springer, New York.

[14] Krykun, I. (2017). Convergence of skew brownian motions with local times at several points that are contracted into a single one. *Journal of Mathematical Sciences*, 221(5):671–678.

[15] LeGall, J. (1984). *One-dimensional stochastic differential equations involving the local times of the unknown process.* Springer, Berlin, Heidelberg.

[16] Lehner, G. (1963). One-dimensional random walk with a partially reflecting barrier. *Ann. Math. Stat.*, 34:405–412.

[17] Lejay, A. (2006). On the constructions of the skew brownian motion. *Probab. Surv.*, 3:413–466.

[18] L'epingle, D. (2009). Boundary behavior of a constrained brownian motion between reflecting-repellent walls.

[19] Linetsky, V. (2005). On the transition densities for reflected diffusions. *Advances in Applied Probability*, 37(2):435–460.

[20] Lions, P. and Sznitman, A. (1984). Stochastic differential equations with reflecting boundary conditions. *Communications on Pure and App. Maths*, 37(4):511–537.

[21] Mazzonetto, S. (2016). *On the exact simulation of (skew) Brownian diffusions with discontinuous drift (Doctoral dissertation, Universität Potsdam).*

[22] Mazzonetto, S. (2019). Rates of convergence to the local time of oscillating and skew brownian motions. *arXiv preprint arXiv:1912.04858.*

[23] Ouknine, Y., Russo, F., and Trutnau, G. (2015). On countably skewed brownian motion with accumulation point. *Electron. J. Probab.*, 20(82):1–27.

[24] Percus, O. (1985). Phase transition in one-dimensional random walk with partially reflecting boundaries. *Adv. Appl. Prob.*, 17:594–606.

[25] Portenko, N. (1976). *Generalized diffusion processes.* Springer, Berlin.

[26] Ramirez, J. (2011). Multi-skewed brownian motion and diffusion in layered media. *Proceedings of the American Mathematical Society*, 139(10):3739–3752.

[27] Sacerdote, L., Tamborrino, M., and Zucca, C. (2016). First passage times of two-dimensional correlated processes: Analytical results for the wiener process and a numerical method for diffusion processes. *Journal of Computational and Applied Mathematics*, 296:275–292.

[28] Taranto, A. and Khan, S. (2020a). Bi-directional grid absorption barrier constrained stochastic processes with applications in finance and investment. *Risk Governance & Control: Financial Markets & Institutions*, 10(3):20–33.

[29] Taranto, A. and Khan, S. (2020b). Drawdown and drawup of bi-directional grid constrained stochastic processes. *Journal of Mathematics and Statistics*, 16(1):182–197.

[30] Taranto, A. and Khan, S. (2020c). Gambler's ruin problem and bi-directional grid constrained trading and investment strategies. *Investment Management and Financial Innovations*, 17(3):54–66.

[31] Taranto, A. and Khan, S. (2021a). Application of bi-directional grid constrained stochastic processes to algorithmic trading. *Journal of Mathematics and Statistics*, 17(1):22–29.

[32] Taranto, A. and Khan, S. (2021b). Hidden geometry of bi-directional grid constrained stochastic processes. *arXiv preprint.*

[33] Taranto, A., Khan, S., and Addie, R. (2020). Iterated logarithm bounds of bi-directional grid constrained stochastic processes. *arXiv Preprint: Modern StochAstic Models & ProbleMs Of Actuarial MaTHematics (MAMMOTH) Conference*, pages 1–21.

[34] Weesakul, B. (1961). The random walk between a reflecting and an absorbing barrier. *Ann. Math. Statist.*, 32:765–769.